A New Method to Assess the Velocity Vector Field in a Beating Heart

WI Meyering*, MA Gutierrez+

*Biomedical Engineering Laboratory (LEB),
University of São Paulo Polytechnic School, São Paulo, Brazil
+Division of Informatics, Heart Institute (InCor),
University of São Paulo Medical School, São Paulo, Brazil

Abstract

The estimation of left ventricle motion and deformation from series of images has been an area of attention in the medical image analysis and still remains an open and challenging research problem. The proper motion tracking of left ventricle wall can contribute to isolate the location and extent of ischemic or infarcted myocardium. We present a complete new methodology to automatically estimate velocity vector fields for a beating heart based on the study of the variation in frequency content in a time series of non-stationary images. The synthetic phantom validation and results obtained from cardiac SPECT images are also presented.

1. Introduction

Left ventricle contractile abnormalities can be an important manifestation of coronary artery disease. Wall motion changes may represent ischemia or infarction of myocardium [1]. The properly extent quantification of regional wall motion abnormality can aid in determining the myocardial effects of coronary artery disease [2-4]. It would also simplify the analysis of wall motion changes after diagnostic and therapeutic interventions and allows comparison of different imaging techniques to assess their diagnostic accuracy. For this reason the tracking of left ventricle wall constitutes a fundamental goal in Nuclear Medicine procedures.

The process to obtain images in Nuclear Medicine involves the detection of the radiation emitted from a patient's organ or region after the injection of a radiopharmaceutical. Using a gamma camera, the detected radiation produce an image indicating the distribution of radionuclide in the body. This distribution represents the projection of a radioactive volume over the detector's face or, after tomographic reconstruction, the radioactive distribution in a volume section or slice.

Some radiopharmaceuticals such as ^{201}Tl and ^{99m}Tc-MIBI can provide information about the myocardium perfusion. Following intravenous injection, these radioactive substances are extracted almost completely from the plasma during the first pass throughout the various tissues. Defects on their distribution in the myocardium indicate a muscle hipoperfusion due to obstruction of the coronary arteries. Electrocardiographic gating of MIBI SPECT images provides the additional ability to determine the severity of abnormalities in wall motion and wall thickening associated with perfusion defects.

This work describes a complete new methodology to automatically estimate velocity vector fields for a beating heart based on the study of the variation in frequency content in a series of non-stationary images as time varies. The synthetic phantom validation and results obtained from cardiac SPECT images are also presented.

2. Methods

The tracking of structures in time series images has been studied by the computer vision community, especially in the areas of non-rigid motion, segmentation and surfacing mapping. The goal is to obtain a displacement field that establishes a correspondence between certain points in the structure at time t and time $t+1$.

Generally speaking, the common methods to obtain velocity vector fields lie within feature matching, gradient and frequency based techniques. These methods have severe shortcomings: **(1)** they are very sensitive to ambiguity amongst the structures to be matched; **(2)** correspondences between different structures in the reference model can suffer from combinatorial explosion; **(3)** derivative estimation introduces noise and some level of filtering is required; **(4)** frequency based methods produce a non-localized velocity vector for each image frame.

In this work, we propose and validate a new methodology to motion detection based on spatial and temporal frequency (STF) analysis. The majors motivations for considering the use of STF representation as a basis for computing velocity vector fields are: **(1)** it is

0276-6547/01 $17.00 © 2001 IEEE

Computers in Cardiology 2001;28:441-444.

used for the description and understanding of signals whose frequency content is changing with time (non-stationary signals). This is the exact case when studying non-rigid motion in a series of images; (2) some investigations on mammalian vision have demonstrated that many neurons in various visual cortical areas of the brain behave as spatiotemporal-frequency band-pass filters [7].

In the field of non-stationary signal analysis, the Wigner-Ville Distribution (WVD) has been used for the representation of speech and image. Jacobson and Wechsler [5, 6] first suggested the use of the WVD for the representation of shape and texture information in images. In particular, they formulated a theory for invariant visual pattern recognition in which the WVD plays a central role.

Given a time-varying image $f(x,y,t)$, its Wigner-Ville Distribution [8] is a 6-dimensional function defined as:

$$W_f(x,y,t,w_x,w_y,w_t) = \int_{-\infty}^{+\infty}\iiint R_f(x,y,t,\alpha,\beta,\tau)\,e^{-j(\alpha w_x+\beta w_y+\tau w_t)}\,d\alpha d\beta d\tau \quad (1)$$

where

$$R_f(x,y,t,\alpha,\beta,\tau) = f(x+\alpha,y+\beta,t+\tau).f^*(x-\alpha,y-\beta,t-\tau) \quad (2)$$

and where * denotes complex conjugation.

For the special case where a time-varying image $f(x,y,t)$ is uniformly translating at some constant velocity (v_x,v_y), the image sequence can be expressed as a convolution between a static image and a translating delta function:

$$f(x,y,t) = f(x,y) * \delta(x-v_x t, y-v_y t) \quad (3)$$

Using the convolution and windowing properties of the Wigner-Ville distribution of $f(x,y,t)$ we obtain

$$W_f(x,y,t,w_x,w_y,w_t) = \delta(v_x w_x + v_y w_y + w_t) W_f(x-v_x t, y-v_y t, w_x, w_y) \quad (4)$$

From (4), the WVD of a linearly translating image with velocity (v_x,v_y) is everywhere zero except in the plane defined by (5) for fixed (v_x,v_y).

$$\{(x,y,t,w_x,w_y,w_t): v_x w_x + v_y w_y + w_t = 0\} \quad (5)$$

Equivalently, for an arbitrary pixel at x,y,t, each local spatiotemporal frequency spectrum of the Wigner-Ville distribution is zero everywhere except on the plane defined by:

$$\{(w_x,w_y,w_t): v_x w_x + v_y w_y + w_t = 0\} \quad (6)$$

From (1) the Wigner-Ville distribution assigns a three-dimensional spatiotemporal-frequency spectrum to each pixel x,y,t, over which the image is defined [6, 7]. However, the WVD assigns a 3D spectrum with interference due cross correlation [8] when more than one frequency is present. In order to smooth the image a filter must be introduced. In this work the Hanning filter was used:

$$h = 0{,}5 * \left[1 - \cos\left(\frac{2\pi n}{N}\right)\right] \quad \text{for} \quad 0 \le n \le N-1 \quad (7)$$

Therefore, given a procedure for estimating the velocity associated with a given STF spectrum, the WVD allows to obtain the space and time varying velocity vector field.

After obtaining the smoothed 3D-frequency spectrum, it is possible to estimate the velocity vector for each pixel by determining the best fitting plane to the points of WVD. The orientation of this plane in the space is also directly related to the pixel velocity. The plane can be obtained through a multiple linear regression [9,10]:

$$z = b_0 + b_1 x + b_2 y + e \quad (8)$$

The equation (8) is a linear regression extension where z is a linear function of two independent variables. The values of the coefficients b_0, b_1, b_2 are achieved by solving the liner system:

$$\begin{bmatrix} n & \sum x_i & \sum y_i \\ \sum x_i & \sum x_i^2 & \sum x_i y_i \\ \sum y_i & \sum x_i y_i & \sum y_i^2 \end{bmatrix} \begin{Bmatrix} b_0 \\ b_1 \\ b_2 \end{Bmatrix} = \begin{Bmatrix} \sum z_i \\ \sum x_i z_i \\ \sum y_i z_i \end{Bmatrix} \quad (9)$$

The coefficients b_1, b_2 are related to the movement on x and y directions, respectively. The quantification of the fitting process can be done by the coefficient of multiple determination (R^2), that measures the proportionate reduction in the total sum of squares associated with the use of the independent variables x and y in the multiple regression model [11]:

$$R^2 = \frac{\sum (\hat{z}_i - \bar{z})^2}{\sum (z_i - \bar{z})^2} \quad (10)$$

where $\hat{z}_i$ and $\bar{z}$ are the estimated and medium value of z, respectively.

3. Results

3.1. Synthetic images

The synthetic image consists of a texture distributed in a grid of 32x32 (figure 1), where dark pixels simulate hot regions in SPECT images.

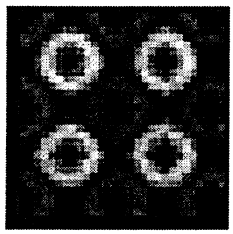

Figure 1: Synthetic image.

Using a Hanning filter, the velocity vector field was obtained after translations and rotations experiments of the synthetic image. The results are shown on table 1 (translations) and table 2 (rotations). Table 1 shows real and estimated velocities in pixels/frame, the standard deviation and the root mean square error (RMSE), measured between the real and the estimated velocities. Table 2 shows real and estimated angular velocity in degrees/frame, the standard deviation and the root mean square error (RMSE).

Table 1. Data for the simulation of translations.

vx	vy	$\hat{v}$ x	$\hat{v}$ y	std	rmse
1	0	0,9012	0	0,0317	11,87
2	0	1,8022	-0,0004	0,0753	12,29
0	1	-0,0001	0,8693	0,0424	16,01
0	2	0,0001	1,7396	0,0835	15,93
1	1	0,9018	0,8562	0,0636	15,32
1	2	0,9050	1,7209	0,1024	16,39
2	1	1,8002	0,8662	0,0920	13,30
1	-2	0,9049	-1,7221	0,1011	16,32
-2	1	-1,8005	0,8655	0,0929	13,33

Table 2. Data for the simulation of rotations.

w	$\hat{w}$	std	rmse
2	1,79	0,0067	23,80
4	3,57	0,0120	22,32
5	4,42	0,0131	21,04
6	5,33	0,0156	20,59
7	6,22	0,0187	20,95
8	7,06	0,0210	21,30
10	8,91	0,0267	20,71
12	10,63	0,0334	21,71
14	12,40	0,0384	21,47
16	14,09	0,0452	22,24
18	15,80	0,0515	22,63
20	17,63	0,0563	21,99

Figure 2 shows the velocity vector field obtained after translation and rotation movements imposed to the synthetic phantom.

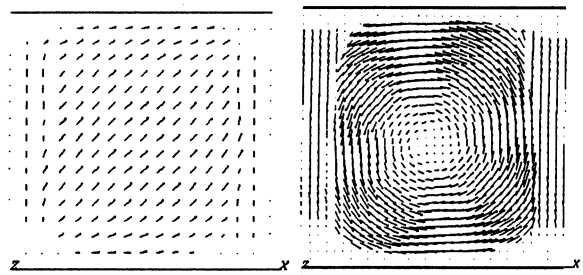

Figure 2: Velocity vector field after translation of 1 pixels/frame in both directions **(left)** and rotation of 6 degrees/frame on counter-clockwise direction **(right)**.

Figure 3 shows the root mean square error (RMSE) obtained along the radii from the center of the image on rotation simulation of 6 degrees/frame. The RMSE is greater at the center of the image due to low tangential velocities and at the edges due to border effect.

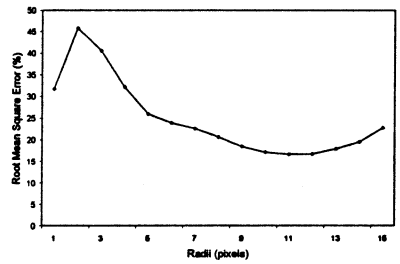

Figure 3: Root mean square error (RMSE) calculated during the rotation of 6 degree/frame.

The errors associated with the velocity measurement are around 14,5% for translation simulations and around 21,7% for rotation simulations. These results show that the methodology performs well for translation and rotation applied to the phantom for the cases shown in the tables 1 and 2.

3.2. Real images

The procedure to estimate the motion was also applied to gated-SPECT perfusion study ^{99m}Tc-MIBI obtained from a dual head rotating gamma camera (ADAC VertexPlus with a LEAP Collimator). The acquisition process is synchronized with the electrocardiogram and the cardiac cycle can be divided into 8 or 16 frames per cycle. A total of 64 projections were obtained over a semi-circular 180° orbit. All projections images were stored using a 64x64, 16 bits matrix. All transverse tomograms were reconstructed with a thickness of one pixel per slice (6,47mm). The volume of transverse tomograms was re-oriented, and sets of slices

perpendicular to the long axis (oblique transverses) and of slices parallel to the long axis (oblique coronals and sagittals) were created.

The velocity vector field was obtained from a series of 2D gated-SPECT slices. Figure 4 depicts the results obtained for one oblique SPECT slice at systole and diastole and the superimposition of the velocity vector field.

The computational time to obtaining the velocity vector field for all pixels in an image with spatial resolution of 32x32 and 32 time frames is 2:40 hours (SUN UltraSparc II-400 MHz with SPECint95=17.4 and SPECfp95=40.6). One way to decrease the computational time is to use a threshold to remove pixels with lower counts (background) and undesired structures. Figure 5 shows the same oblique SPECT slice computed with a threshold of 30%. In this case, the computational time was reduced to 35 minutes on the same computer.

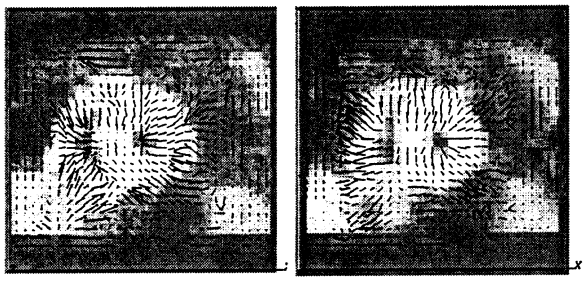

Figure 4: Oblique SPECT slice at systole **(left)** and diastole **(right)**, superimposed by the velocity vector field

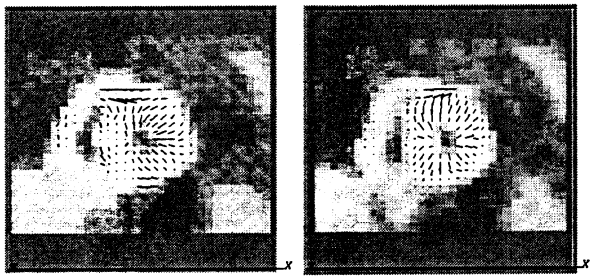

Figure 5: The velocity vector field calculated over the pixels with a threshold of 30%.

4. Conclusions

This work described a new methodology to determine velocity vector fields in cardiac images based on spatial and temporal frequency (STF) analysis. The majors motivations for considering the use of STF representation as a basis for computing non-rigid motion are: **(1)** it is used for the description and understanding of signals whose frequency content is changing with time (non-stationary signals). This is the exact case when studying non-rigid motion in a series of images; **(2)** some investigations on mammalian vision have demonstrated that many neurons in various visual cortical areas of the brain behave as spatiotemporal-frequency band-pass filters.

The method was applied in synthetic images in experiments involving translation and rotation and in real images of a gated-SPECT study yielding the velocity vector that describe the corresponding motion.

In order to decrease the computational time a threshold was applied to the cardiac image reducing the number of pixels that has to be calculated. This solution has decreased the computational time in about 20% of the original time.

Acknowledgements

This work has been supported by Grant n°.97/14207-1 of the Foundation of Aid for Research of São Paulo State (FAPESP) and the Zerbini Foundation.

References

[1] Marcassa C, et al. A new method for noninvasive quantitation of segmental myocardial wall thickening using Tc-99m-2-methoxy-isobutyl-isonitrile: scintigraphic results in normal subjects. Journal of Nuclear Medicine 1990; 173-177:31.

[2] Faber T, et al. Quantification of three-dimensional left ventricular segmental wall motion and volumes from gated tomographic radionuclide ventriculograms. Journal of Nuclear Medicine 1989; 638-649:30.

[3] Gelberg H, et al. Quantitative left ventricular wall motion analysis: A comparison of area, chord and radial methods. Circulation 1979; 991-1000:59.

[4] Creswell LL, Pasque MK and Vannier MW. Three-dimensional cardiac magnetic resonance imaging. American Journal of Cardiac Imaging 1993;195-208:7.

[5] Jacobson L and Wechsler H. Joint spatial/spatial-frequency representation. Signal Processing 1988; 14:37-68.

[6] Jacobson L and Wechsler H. Derivation of optical flow using a spatiotemporal-frequency approach. Computer Vision, Graphics and Image Processing 1987; 38:29-65.

[7] Laplante PA and Stoyenko AD. Real-time imaging: theory, techniques and applications. IEEE Press, 1996.

[8] Cohen L. Time-frequency analysis. New Jersey, Prentice Hall PTR, 1995.

[9] Chapra SC and Canale RP. Numerical methods for engineers with programming and software applications. 3rd edition. WCB/McGraw-Hill, 1998.

[10] Kleinbaum DG, Kupper LL, Muller KE. Applied regression analysis and other multivariable methods. 2nd edition. Boston, PWS-KENT Publishing Company, 1988.

[11] Neter J, Wasserman W, Whitmore GA. Applied statistics. Allyn and Bacon Inc,1979.

Address for correspondence.
Wietske Ineke Meyering
Av. Dr. Eneas de Carvalho Aguiar, 44
05403-000 São Paulo, SP, Brazil
E-mail wietske.meyering@incor.usp.br